
Reagents and physico-chemical methods

In this chapter an outline of the materials, procedures and various physico-chemical methods employed are presented. Some basic aspects of Co(II) and Ni(II) systems in general are also included in this chapter.

3.1 Reagents

The metal salts used for the synthesis of the complexes were BDH grade samples. The ligands used for the preparation of the parent 4-coordinated systems were 2-mercaptobenzothiazole (mbtH), 2-mercaptobenzoxazole (mboH) and 2-mercaptobenzimidazole (mbmH) obtained from E-Merck. The Lewis-bases used for the present study involving pyridine, 4-aminopyridine, 4,4'-bipyridine, and pyrazine were either BDH, Fluka or Merck samples. The solvents used for the present study were of BDH make.

3.2 Preparative Details

3.2.1 Preparation of 4,4'-azopyridine

4,4'-Azopyridine was prepared by oxidative coupling of 4-aminopyridine with hypochlorite with modification of reported procedure.^(1,2) A 100ml aliquot of a cold solution of 4-aminopyridine (5g) in water was added dropwise to

300ml of 10% NaOCl solution. The mixture was stirred at 0°C for 1h to get an orange precipitate. The solid was filtered and collected with the diethyl ether extract of the aqueous solution (filtrate). The clear ether solution was dried with anhydrous MgSO₄. On removing the solvent by evaporation the crude product of 4,4'-azopyridine was obtained as orange solid. This was purified by column chromatography on basic Al₂O₃ using acetone/hexane (1:10) mixture as the eluent. The compound was further purified by recrystallisation from hot water to get long needle-like orange coloured product.

3.3 Elemental Analysis

3.3.1 Estimation of Nickel

For estimating nickel (II) ion, 0.1g of the complex after careful pyrolysis was digested with conc.HCl followed by conc.HNO₃. The solution obtained after digestion was evaporated to dryness and the residue was extracted with distilled water. It was then diluted to 50ml and 25g of murexide indicator was added followed by 5ml of 1M NH₄Cl solution. Ammonia solution was then added to this till pH was raised to 7, by the yellow colour of the solution. It was then titrated against standard EDTA solution. Near the end point, 5ml of conc. NH₃ was added till the pH was 10 and the titration continued till the colour changed to violet.⁽³⁾

3.3.2 Estimation of Cobalt

About 0.1g of the complex was digested with conc. H₂SO₄ followed by conc. HNO₃. A few drops of perchloric acid was also added to the resulting solution. The clear solution obtained was evaporated to dryness and the residue was then extracted with 50ml of distilled water. Hexamine buffer was added to the resulting solution till pH was 6. It was then titrated against standard EDTA solution using xylenol orange indicator till the colour changed from red to yellow.⁽³⁾



3.3.3 Estimation of Vanadium

The vanadium content of the complex was determined volumetrically using decinormal KMnO_4 solution as an oxidising agent in the presence of sulphurous acid. A 100mg sample of the compound was placed in a silica crucible, decomposed by gentle heating and then by adding 1-2 ml of conc. HNO_3 , two to three times. An orange coloured mass (V_2O_5) was obtained after decomposition and complete drying. It was dissolved in minimum amount of dil. H_2SO_4 and the solution so obtained was diluted with distilled water to 100ml in a measuring flask. The amount of vanadium in the sample solution was calculated^(4,5) using the standard relationship given below.

1ml of 0.1N $\text{KMnO}_4 \approx 0.005094\text{g}$ vanadium

3.3.4 Estimation of Carbon, Hydrogen and Nitrogen

The determination of the percentage of carbon, hydrogen and nitrogen in these complexes was carried out using Heracus CHN rapid analyser.

3.4 Spectral Methods

IR spectra

IR spectra provide a useful tool to study the bonding features of all the types of compounds especially coordination compounds. During complex formation the ligands get coordinated to the central metal atom or ion. The newly formed metal-ligand bonds consequently change the electronic structure, the state of energy and the symmetry of the complexes. These changes affect the vibrational modes of various bonds in the ligand and consequently change the vibrational spectrum too. The new complex will perform new vibrations which are not exhibited by the free ligands. The structure, symmetry of the complex molecule and the strength of the coordinate bonds will also affect the vibrational spectrum of these complexes. Because of these reasons infra-red spectra can be considered as an important tool for the analysis of coordination compounds.



In the present study, the infra-red spectra were recorded using Shimadzu IR-470 Spectrophotometer operating in the range 4000-400 cm^{-1} using KBr pellet technique.

Electronic spectra

A Shimadzu-UV-160A Spectrophotometer operating in the spectral range 1100-200nm was used for electronic spectral studies. The spectra were recorded using Nujol mull of the solid samples.

ESR spectra

The ESR spectra of all vanadyl adducts were recorded using E-12 Varian Spectrophotometer by availing the facility at RSIC Bombay. The measurements were carried out at LNT in toluene or toluene + methanol (1:1) mixture. The theoretical aspects of ESR especially concerning VO^{2+} species are discussed in Chapter 9.

3.5 Coordination Chemistry of Cobalt

The most common oxidation states of cobalt are +2 and +3. Few Co(IV) and Co(V) compounds also exist;⁽⁶⁾ golden yellow Cs_2CoF_6 , red brown Ba_2CoO_4 and blue black K_3CoO_4 . Most simple salts exist in the Co(II) oxidation state and crystallise from aqueous solution as $\text{CoX}_2 \cdot 6\text{H}_2\text{O}$ or $\text{CoX}_2 \cdot 4\text{H}_2\text{O}$. Most Co(II) salts in aqueous solution readily dissociates to give the $[\text{Co}(\text{OH}_2)_6]^{2+}$ ion which is pale pink. $[\text{Co}(\text{H}_2\text{O})_6]^{3+}$ is possible in very strong acids, which is blue in colour and is rapidly reduced by water to $[\text{Co}(\text{H}_2\text{O})_6]^{2+}$ liberating oxygen.

Co(II) complexes adopt two major stereochemistries, six-coordinate distorted octahedral and tetrahedral although a few low spin square planar systems are known [Co(Phthalocyanines), Co(Salen)-type Schiff bases] as well as some five-coordinated systems $[[\text{Co}(\text{CN})_5]^{3-}$ is square pyramidal with one unpaired electron; and $[\text{CoBr}(\text{N}(\text{C}_2\text{H}_4\text{NMe}_2)_3)]^+$ is trigonal bipyramidal with three unpaired electrons). Octahedral- tetrahedral stereochemistries are



often found in equilibrium and in aqueous solution even $[\text{Co}(\text{H}_2\text{O})_6]^{2+}$ has a small amount of $[\text{Co}(\text{H}_2\text{O})_4]^{2+}$ present.

The d^7 electronic configuration is that most favored to form the tetrahedral as opposed to the octahedral stereochemistry. Ligand polarizability as well as ligand size are important factors, with the more polarizable ligands (eg., I, P, As, aromatic N donors) favouring tetrahedral structures. Most O and N (amine) donors, however favour octahedral coordination. Octahedral Co(II) complexes are pink to violet in colour (absorption $\sim 500\text{nm}$), whereas tetrahedral complexes are more intensely blue ($\sim 600\text{nm}$). The colour of octahedral Co(II) is dominated by the ${}^4\text{T}_{1g}(\text{F}) \rightarrow {}^4\text{T}_{1g}(\text{P})$ transition (ν_3), with the two lower energy transitions (to ${}^4\text{T}_{2g}(\text{F})$ and ${}^4\text{A}_{2g}(\text{F})$ levels) occurring in the near IR and visible regions (weak) of the spectrum respectively.⁽⁷⁾

The T ground term results in temperature-dependent orbital contributions to the magnetic moment, with values (4.8-5.2BM) falling off appreciably with decreasing temperature. Tetrahedral Co(II) is dominated by the broad and intense ν_3 transition ${}^4\text{A}_2(\text{F}) \rightarrow {}^4\text{T}_1(\text{P})$ with the lower energy ν_1 and ν_2 transitions occurring in the IR (to ${}^4\text{T}_2(\text{F})$, $3000\text{-}5000\text{cm}^{-1}$, to ${}^4\text{T}_1(\text{F})$, $5000\text{-}8000\text{cm}^{-1}$). The spin only moment of 3.87BM for the tetrahedral ligand field is modified by mixing the lower energy ${}^4\text{T}_2(\text{F})$ level into the ground ${}^4\text{A}_2$ term via spin orbit coupling, and this results in greater than spin only magnetic moments (15-25%) depending on the ligand; the moment is temperature independent in this case.

Of the oxides, only CoO and Co_3O_4 are known with certainty. CoO (Green) is easily prepared from the metal and oxygen above 900°C , or by heating Co(II) salts in oxygen. Many sulphides of cobalt are known but few are fully characterised. CoS_2 adopts the iron pyrites structure with discrete S_2^{2-} units and Co_3S_4 adopts the spinal structure. Various cobalt deficient (Co_{1-x}S) sulphides are known and these adopt the NiAs structure.

3.6 Coordination Chemistry of Nickel

Nickel compounds have been found to occur with the metal in oxidation states varying from -1 to +4.⁽⁸⁾ However, comparatively very few compounds



corresponds to the lowest (-1) and to the higher (+3, +4) oxidation states. Ni(-1) has been claimed to be formed only in a few organometallic compounds.⁽⁹⁾

The reported Ni(0) complexes are all diamagnetic which show that the ligand stabilise the 1S ($3d^{10}$) configuration relative to the other ones.⁽¹⁰⁾ Ni(+1) complexes are also comparatively rare similar to Ni(-1) and are paramagnetic (d^9 configuration, $\mu_{\text{eff}} = 1.7\text{-}2.4$ BM).

The overwhelming majority of Ni(II) complexes have coordination numbers of four, five or six. Complexes with coordination numbers of 3, 7 and 8 are still quite rare. In almost all its six-coordinated complexes of nickel (II) has a pseudo octahedral stereochemistry with a spin triplet as ground state (high spin configuration). The magnetic moments of octahedral Ni(II) usually lie between 2.9 and 3.3 BM and the temperature dependence of the magnetic susceptibilities follow Curie -Weiss law.

Five-coordination is also now quite common in Ni(II) complexes and many polydentate ligands such as polyamines, salicylaldimine polyarsines and polyphosphines have been designed with the purpose of favouring this stereochemistry.^(11,12)

However five-coordinate complexes with monodentate ligands $[\text{Ni}(\text{CN})_5]^{3-}$ and $[\text{Ni}(\text{OAsMe})_5]^{2-}$ are also known. The five coordinated Ni(II) complexes have structure which are generally near to one of the two limiting geometries, namely the square pyramid and trigonal bipyramid. The electronic ground state of Ni (II) in five-coordinated complexes can neither a spin singlet or a spin triplet. Spin singlet corresponds to low spin configuration while spin triplet to high spin configuration.

The majority of 4-coordinated nickel (II) complexes are square planar and invariably diamagnetic, whereas pseudo tetrahedral complexes which are always paramagnetic are relatively rare. It is in general found that ligands with weaker donor strength favour a pseudotetrahedral structure, whereas ligands with higher donor strength tend to produce square planar structure. It must also be born in mind that ligands which contains bulky substituents on the donor atoms may prevent a planar structure due to steric hindrance, and



a distorted tetrahedral structure may become preferred.⁽¹³⁾ Nickel (II) in tetrahedral geometry has an orbitally degenerate ground state and the magnetic moments are expected to be substantially higher than those of six-coordinate complexes because of large orbital contribution. The magnetic moments are usually found to be in the range 3.3 - 4.0BM at room temperature.

Strong Ni-Ligand interaction stabilise planar configuration in 4-coordinated Ni(II) complexes. Planar complexes of Ni(II) are often red or yellow owing to an absorption around 500nm. The majority of square-planar complexes are formed by interacting either chelating ligands or tetradentate macrocyclic ligands with Ni(II). Porphyrins and phthalocyanines also stabilise square planar structure. Fig.3.1 shows the d-orbital splitting pattern for tetrahedral, square planar and octahedral Ni²⁺ complexes.

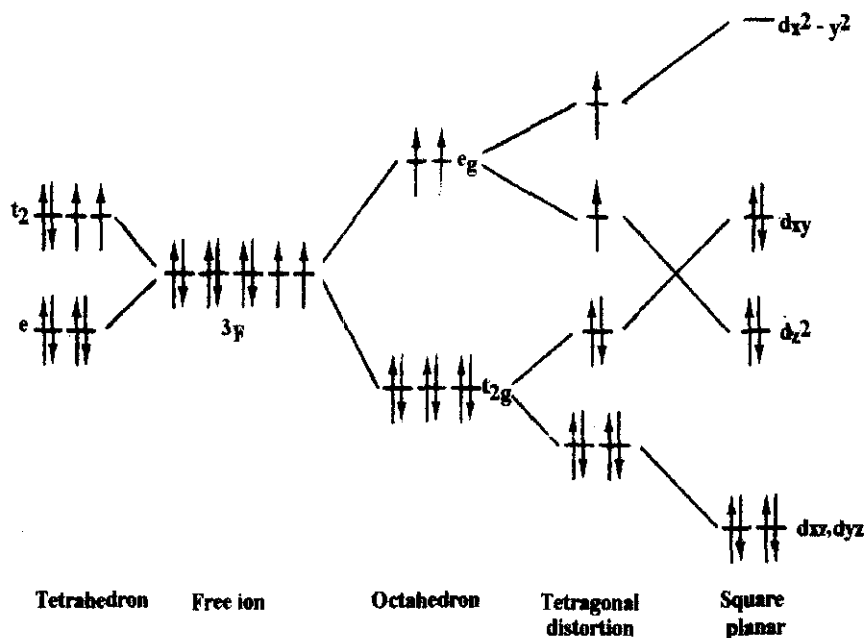


Fig.3.1 d-orbital splitting pattern for tetrahedral, square planar and octahedral Ni²⁺.

Another common feature of square planar Ni(II) complexes is their ability to coordinate extra ligands in solution to set up equilibria between four, five and six-coordinated complexes. Thus diamagnetic square planar complexes can be transformed in coordinating solvents or in the presence of extra ligands to paramagnetic octahedral Ni(II) species.

The electronic spectral features of nickel complexes have been thoroughly reviewed. Tetrahedral complexes are usually highly coloured due to their expected d-d transition from ${}^3T_1(F)$ to ${}^3T_2(F)$ (ν_1), to ${}^3A_2(F)$ (ν_2) and to ${}^3T_1(P)$ (ν_3), respectively. But the observed spectra tend to be complicated by spin-orbit coupling effects.

These d-d transitions due to ${}^3A_{2g}(F)$ to ${}^3T_{2g}(F)$ (ν_1), ${}^3T_{1g}(F)$ (ν_2), and to ${}^3T_{1g}(P)$ (ν_3), would be observed for Ni(II) in octahedral field. The simplified Orgel diagram for tetrahedral and octahedral Ni(II) is shown in Fig.3.2. Ni(II) square planar complexes have a single band in the range 18000-25000 cm^{-1} due to transition for ${}^1B_{1g} \rightarrow {}^1A_{1g}$.⁽¹⁴⁾

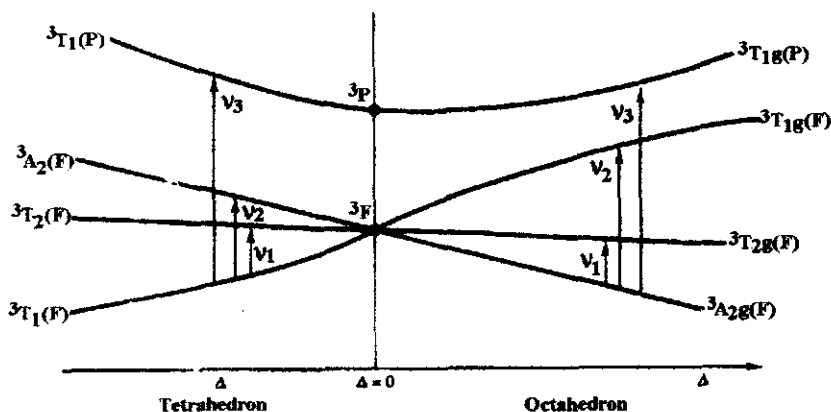


Fig.3.2 The simplified Orgel diagram for tetrahedral and octahedral Ni(II)

3.7 Magnetic Susceptibility Measurements

Magnetochemistry is used to investigate the magnetic properties of transition metal complexes. Magnetic moment can provide information about the oxidation state of the metal ion, electronic structure and symmetry properties of the complexes. This also would give a clear idea about the number of unpaired electrons in the central metal atom or ion in the complex.

In first row transition metals, the spin only magnetic moment can be calculated using the equation.

$$\mu_{(s.o)} = [4S(S+1)]^{1/2} \text{-----(3.1)}$$



The magnetic susceptibilities of the complexes were measured at room temperature using a Gouy magnetic balance. The Gouy tube was standardised using mercury(II)tetrathiocyanatocobaltate(II). Diamagnetic corrections for the rest of the molecules were computed from Pascal's constants. Gram susceptibility was calculated using the formula.

$$\chi_g = \frac{\alpha + \beta E}{W} \quad \text{-----(3.2)}$$

where α = air displacement constant, β = Gouy tube constant

E = change in weight in mg, W = Weight of the sample in gram

The effective magnetic moments, μ_{eff} , were calculated from corrected molar magnetic susceptibility, χ_m^* .

$$\chi_m = \chi_g \cdot \text{mol wt.} \quad \text{-----(3.3)}$$

$$\chi_m^* = \chi_m + D \quad \text{-----(3.4)}$$

where, D is the diamagnetic correction.

$$\mu_{\text{eff}} = 2.84 \sqrt{\chi_m^* \cdot T} \text{ BM} \quad \text{-----(3.5)}$$

For the present study the magnetic susceptibilities were measured on a Sartorius semimicro Gouy balance at room temperature (28 ± 2)°C. The fields were calculated using mercury (II) tetrathiocyanato cobaltate (II) as calibrant.

3.8 Thermal Analysis

The term thermal analysis incorporates those techniques in which some physical parameters of the system is determined and/or recorded as a function of temperature. Based on this various techniques of thermal analyses were used. Among these techniques thermogravimetry (TGA) is an important one.

Thermogravimetry is a technique where by the weight or mass of a substance in an environment heated or cooled at a controlled rate is



recorded as a function of temperature. Thermogravimetric analysis provides the analyst a quantitative measurement of any weight change associated with a transition. The changes in mass are as a result of the rupture and or formation of chemical bonds at elevated temperature and evolution of some volatile products. Thermogravimetric curves are characteristic for a given compound because of unique sequence of physico-chemical reactions which occur over definite temperature ranges. These changes are a function of its temperature dependent molecular structure. From such curves it is possible to explain the thermodynamics and kinetics of various chemical reaction mechanisms, the intermediates and the final reaction products obtained.

Mainly two methods are usually employed in thermogravimetry: (1) Isothermal or static method where the mass of the sample is recorded as a function of time at constant temperature (2) Non-isothermal or dynamic method where the sample is heated in an environment whose temperature is changing in a linear rate.

From non-isothermal studies of samples developed in the present study the following aspects have been studied.

a) Phenomenological aspects

From this it is possible to find out the thermal stability of a substance, the procedural temperature (T_i), the final temperature (T_f), the temperature of maximum loss (T_s), the physico-chemical reactions which occur over definite temperature ranges, the intermediate substance formed and the final products of the reaction.

b) Kinetic aspects

One of the most important applications of thermogravimetry involves the study of reaction kinetics and mechanism of solid state thermal decomposition reactions. The reaction rate of a solid thermal decomposition can be expressed by the general equation,⁽¹⁵⁾



$$\frac{d\alpha}{dt} = A \cdot \exp\left(\frac{-E}{RT}\right) \cdot f(\alpha) \quad \text{-----(3.6)}$$

where, A = Pre-exponential factor, t = time, and α = fractional decomposition.
E = activation energy. The f(α)-depends on the mechanism of the reaction.

$$\alpha = \frac{W_o - W}{W_o - W_t} \quad \text{-----(3.7)}$$

where, W_o , W and W_t are initial, actual and final sample weights respectively.

When the temperature of the sample is increased at a constant rate of

$\phi = \frac{dT}{dt}$, we can write

$$\frac{d\alpha}{dT} = \frac{A}{\phi} \cdot \exp\left(\frac{-E}{RT}\right) \cdot f(\alpha) \quad \text{-----(3.8)}$$

or,
$$\frac{d\alpha}{f(\alpha)} = \frac{A}{\phi} \cdot \exp\left(\frac{-E}{RT}\right) dT \quad \text{-----(3.9)}$$

On integration,

$$g(\alpha) = \int_0^\alpha \frac{d\alpha}{f(\alpha)} = \frac{A}{\phi} \int_0^T \exp\left(\frac{-E}{RT}\right) dT \quad \text{-----(3.10)}$$

where g(α) is the integrated form of f(α)

or,
$$\ln g(\alpha) = \frac{-E}{RT} + \ln \frac{AR}{\phi E} \quad \text{-----(3.11)}$$

Plotting the LHS of equation 3.11 against 1/T should give a straight line with a slope of $-E/R$ irrespective of g(α) values employed. The kinetic parameters were also calculated from the same linear plot. The value of E and A were calculated from the slope and intercept respectively. The entropy of activation ΔS was calculated from the equation,



$$A = \left(\frac{K.T_s}{h} \right) \exp\left(\frac{\Delta S}{R} \right) \quad \text{-----(3.12)}$$

where k = Boltzmann constant, h = Planck's constant ΔS = entropy of activation.

c) Mechanism of reaction from non-isothermal TG

Deduction of the mechanism of reaction from non-isothermal methods has been discussed by Sestak and Berggren.⁽¹⁶⁾ Kinetic parameters are evaluated from non-isothermal TG curves by the application of Arrhenius equation. The usual non-mechanistic kinetic equation are extension of those used in homogeneous kinetics, where it is assumed that $f(\alpha) = (1-\alpha)^{1-n}$ and mechanistic kinetic studies are based on the assumption that the form of $g(\alpha)$ depends on the reaction mechanism. A series of $f(\alpha)$ forms are proposed and the mechanism is obtained from the one that gives the best representation of the experimental data.

Four non-mechanistic methods are usually used for the calculation of kinetic parameters from the TG curve. The forms of these equations used are given below, where the term $g(\alpha)$ has been introduced for convenience and defined as

$$g(\alpha) = \frac{1 - (1 - \alpha)^{1-n}}{1 - n} \quad \text{-----(3.13)}$$

1. Coats-Redfern equation ⁽¹⁵⁾

$$\ln \left[\frac{g(\alpha)}{T^2} \right] = \ln \left[\frac{AR}{\phi E} \left(1 - \frac{2RT}{E} \right) \right] - \frac{E}{RT} \quad \text{-----(3.14)}$$

2. MacCallum-Tanner equation ⁽¹⁷⁾

$$\log_{10} g(\alpha) = \log_{10} \left[\frac{AE}{\phi R} \right] - 0.485 E^{0.435} - \frac{[0.449 + 0.217E]10^3}{T} \quad \text{-----(3.15)}$$

3. Horowitz-Metzger equation ⁽¹⁸⁾

$$\ln g(\alpha) = \ln \left(\frac{ART_s}{\phi E} \right) - \frac{E}{RT_s} + \frac{E\theta}{ET_s^2} \quad \text{-----(3.16)}$$



4. MKN equation ⁽¹⁹⁾

$$\ln\left(\frac{g(\alpha)}{T^{1.9215}}\right) = \ln\left(\frac{AE}{\phi R}\right) + 3.7721 - 1.9215 \ln E - 0.12039\left(\frac{E}{T}\right) \text{-----(3.17)}$$

where α = fraction of decomposition, n = Order parameter, T = Temperature in Kelvin, A = Pre-exponential parameter, ϕ = Heating rate in $^{\circ}\text{C min}^{-1}$, E = Activation energy, R = Gas constant, T_s = DTG peak temperature, $\theta = (T-T_s)$, M = Mass loss in TG experiment, a = Area of DSC curve at time t and after the completion of the reaction

The kinetic parameters were calculated from the linear plot of the LHS of the kinetic equation against $1/T$ for equations 3.14, 3.15 and 3.17 and against θ for equation 3.16. The value of E and A were calculated from the slope and intercept respectively.

The Coats-Redfern equation (eqn. 3.14) was used for solving the exponential integral in the present study because it is one of the best approaches recommended by several authors.⁽²⁰⁻²²⁾ Satava⁽²³⁾ listed nine probable reaction mechanisms from the Coats-Redfern equation which are given in Table. 3.1

Table 3.1 Mechanism based equations

Eqn. No.	Form of $g(\alpha)$	Rate Controlling process
1	α^2	One-dimensional diffusion
2	$\alpha + (1-\alpha)\ln(1-\alpha)$	Two-dimensional diffusion
3	$\{1-(1-\alpha)^{1/3}\}^2$	Three-dimensional diffusion, spherical symmetry; Jander equation
4	$\frac{2}{3}\left(1-\frac{2}{3}\alpha\right)-(1-\alpha)^{2/3}$	Three dimensional diffusion, spherical symmetry; Ginstling-Brounshtein equation
5	$-\ln(1-\alpha)$	Random nucleation, one nucleus on each particle; Mampel equation
6	$[-\ln(1-\alpha)]^{1/2}$	Random nucleation; Avrami equation I
7	$[-\ln(1-\alpha)]^{1/3}$	Random nucleation; Avrami equation II
8	$1-(1-\alpha)^{1/2}$	Phase boundary reaction, cylindrical symmetry
9	$1-(1-\alpha)^{1/3}$	Phase boundary reaction, spherical symmetry



References

1. J.P. Lawray, M. Tourrel-Paggis, J.F. Lipsker, V. Masrvand and C. Joachin, *Inorg. Chem.*, **30** (1992) 1033
2. E.V. Brown, G.R. Granneman, *J. Am. Chem. Soc.*, **97** (1976) 621.
3. A.I. Vogel, *A Textbook of Quantitative Inorganic Analysis*; ELBS London (1978).
4. N.H. Furman, "Standard Methods of Chemical Analysis" 6th Ed., Vol. **1** (1962) 1211.
5. R.C. Maurya, D.D. Mishra, and V.Pillai, *Synth. React. Inorg. Met-Org. Chem.*, **25(7)** (1995) 1127.
6. W. Levason and C.A. McAuliffe, *Coord. Chem. Rev.*, **12** (1974) 151.
7. R.L. Carlin, *Transition Met. Chem.*, **1** (1965) 1.
8. F.A. Cotton and G. Wilkinson, 'Advanced Inorganic Chemistry' 4th Ed. Wiley-Interscience, New York (1980) 785.
9. K. Nag and A. Chakravothy, *Coord. Chem. Rev.*, **33** (1980) 87.
10. L. Malatesta and S. Cenini, 'Zero-valent Compounds of metals', Academic Press, London (1974).
11. R.L. Orioli, *Coord. Chem. Rev.*, **6** (1971) 285.
12. R. Morassi, I. Bertini and L. Sacconi, *Coord. Chem. Rev.*, **11** (1973) 343.
13. E. Uhlig, *Coord. Chem. Rev.*, **10** (1973) 227.
14. A.B.P. Lever, 'Inorganic Electronic Spectroscopy', Elsevier, Amsterdam (1968).
15. A.W. Coats and J.P. Redfern, *Nature*, **201** (1964) 68.
16. J. Sestak and G. Berggren, *Thermochim. Acta*, **3** (1971) 1.
17. J.R. Mac - Callum and J. Tanner, *Eur. Polym. J.*, **6** (1970) 1033.
18. H.H. Horowitz and G. Metzger, *Anal. Chem.*, **35** (1963) 1964.
19. P.M. Madhusudanan, K. Krishnan and K.N. Ninan, *Thermochim. Acta*, **97** (1986) 189.
20. M.D. Juddo and M.T. Pope, *J. Therm. Anal.*, **4** (1972) 31.
21. J. Zsako, *J. Therm. Anal.*, **5** (1973) 239.
22. Y.M. Gorbachev, *J. Therm. Anal.*, **8** (1975) 349.
23. V. Satava, *Thermochim. Acta*, **2** (1971) 423.

